



UNIVERSITATEA NAȚIONALĂ DE ȘTIINȚĂ ȘI
TEHNOLOGIE POLITEHNICĂ DIN BUCUREȘTI

FACULTATEA ȘTIINȚA ȘI INGINERIA
MATERIALELOR



Autoare: Ing.Cristina Maria IORDACHE (GHEORGHE)

**CORRELATION BETWEEN STRUCTURE-
MECHANICAL CHARACTERISTICS-
BIODEGRADATION-CAVITATION IN
BIOMEDICAL ALLOYS FROM THE ZnMg(Fe)
SYSTEM**

PhD supervisors: Prof. habil. dr. ing. Brândușa GHIBAN

Prof. dr. ing. Ilare BORDEAȘU

București 2024

CONTAINED

THANKS	3
CHAPTER 1 - DEVELOPMENT OF BIODEGRADABLE ZINC ALLOYS FOR BIOMEDICAL APPLICATIONS	6
1 INTRODUCTION	6
1.2. Manufacture and post-thermomechanical takeover of Zn-based biodegradable metals	9
1.2.1. Manufacture of Zn-based MBs	9
1.2.2. Post-thermomechanical processing	11
1.3. Microstructure, texture evolution and mechanical properties of Zn-based alloys	12
1.3.1. Zn alloys containing nutrients	12
1.3.2. Zn alloys containing crucial elements	15
1.3.3. Zn alloys containing other elements	17
1.4. Tribological properties of Zn alloys	19
1.5. Corrosion mechanisms and degradation behaviours of pure Zn and ZnMg(Fe) alloys	20
1.5.1. In vitro degradation of Zn-based materials	22
1.5.2. In vivo degradation behaviour of Zn-based materials	24
1.6. Zn-based composition	25
1.6.1. Bioceramic reinforcements in Zn-based composites	26
1.6.2. Carbon reinforcements in Zn-based composites	28
CHAPTER 2 - MATERIAL, RESEARCH METHODOLOGY AND EXPERIMENTAL PROGRAM OF THE RESEARCH OF THIS DOCTORAL THESIS	30
2.1. Material and equipment used in the experimental programme	30
2.2. The experimental program carried out within the present doctoral thesis	35
CHAPTER 3- PHYSICO-MECHANICAL AND STRUCTURAL CHARACTERIZATION OF EXPERIMENTAL ZINC ALLOYS COMPARED TO PURE ZINC	37
3.1. Physico-mechanical behavior of zinc alloys in the ZnMg(Fe) system compared to pure zinc	37
3.2. Metallographic analysis of zinc alloys in the ZnMg(Fe) system, compared to pure zinc	52
3.3 Scanning electron microscope analysis of ZnMg(Fe) alloys	61
CHAPTER 4 - CORROSION BEHAVIOR IN HUMAN-SIMULATED ENVIRONMENTS OF ZINC-BASED ALLOYS.	65

CORROSION MECHANISMS AND BIODEGRADATION BEHAVIOR	
4.1. General	65
4.2. Experimental results	67
4.3. Discussions and interpretation of the results regarding the biodegradation behavior of experimental alloys compared to the literature	74
CHAPTER 5 - CAVITATIONAL EROSION BEHAVIOR OF EXPERIMENTAL ZINC ALLOYS IN THE ZnMg(Fe) system	77
CHAPTER 6 - FRACTOGRAPHIC ANALYSIS OF CAVITATIONALLY ERODED SURFACES OF EXPERIMENTAL SPECIMENS MADE OF BIODEGRADABLE ALLOYS FROM THE ZnMg(Fe) system	101
CHAPTER 7 - CONCLUSIONS. ORIGINAL CONTRIBUTIONS. PROSPECTS FOR FUTURE RESEARCH	109
A. Conclusions drawn from documentary research	109
B. Conclusions drawn from our own experimental research	111
C. ORIGINAL CONTRIBUTIONS	117
D. PROSPECTS FOR FUTURE RESEARCH	118
BIBLIOGRAPHY	119
LIST OF OWN PUBLICATIONS	134

CHAPTER 1

DEVELOPMENT OF BIODEGRADABLE ZINC ALLOYS FOR BIOMEDICAL APPLICATIONS

Engineered or natural materials that are used to supplement the functions of living tissue are known as biomaterials and have been used as implant materials for a long time in the field of medical science [1-4]. Iron-based (Fe), zinc (Zn) and magnesium (Mg)-based materials have been extensively investigated as potential MB for orthopedic applications [15,22,31,35,37-44]. The microstructure of Zn alloys mainly contains one phase as a matrix (solid solution α -Zn) and the second phase called the intermetallic phase, which is generally hard and brittle. The mechanical properties of Zn alloys are significantly influenced by these intermetallic phases and their fractions of volume, size and distribution in the Zn solid solution matrix; and these microstructural characteristics depend on the methods of manufacture and processing [35]. Zn is known as the "calcium" of the 21st century due to its many important biological roles in the body, including nucleic acid metabolism, stimulation of new bone formation. Fig. 1 shows an

illustration of various in vivo studies using Zn-based materials for potential clinical applications

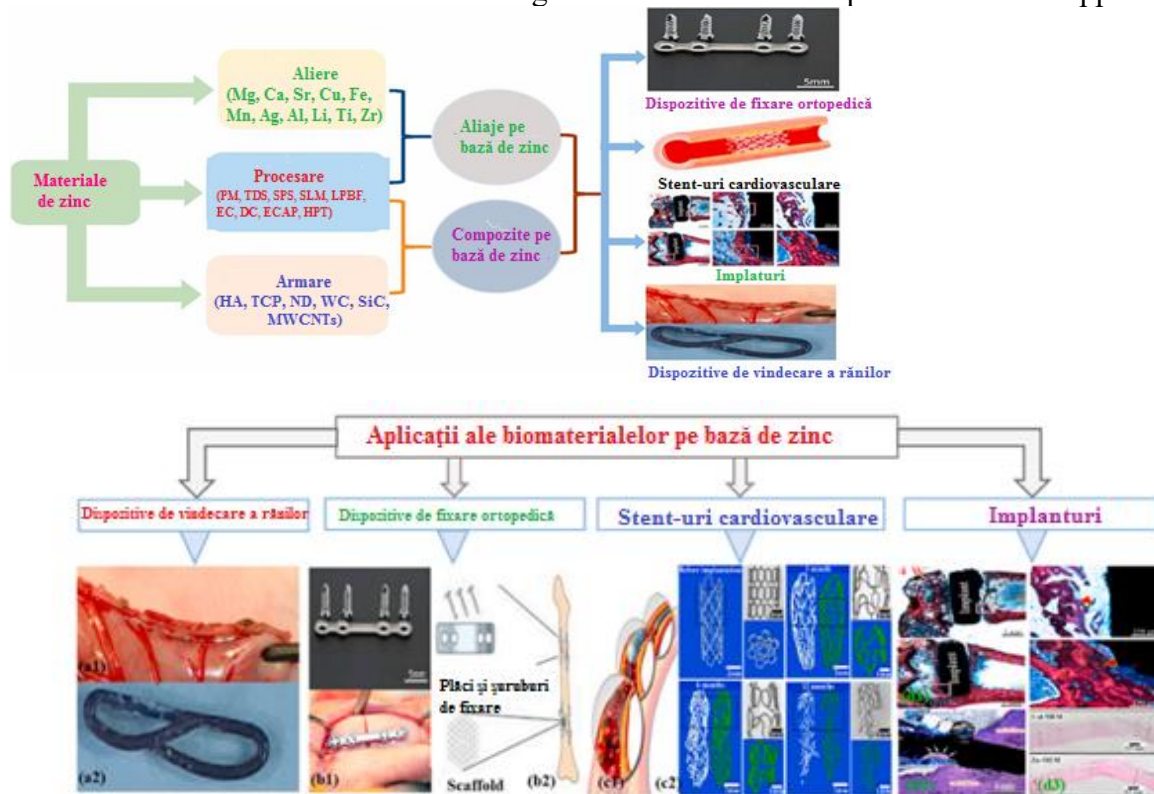


Fig.1. Potential biomedical applications of Zn-based materials: (a1) discontinuous line made of Zn alloy [80], (a2) macroscopic appearance of Zn alloy staples [80], (b1) Zn alloy plate and screws and fixed mandibular bone fractures immediately after surgery [81], (b2) Zn-based fixative plates, porous screws and scaffolds providing temporary mechanical support for bone tissue regeneration [82], (c1) ilustrare schematică a implantării stentului într-un vas coronarian [83], (c2) selected 2D and 3D micro-CT images of Zn stents after different implantation time [84], (d1) histological characterization of hard tissue sections at implant sites for the Zn-5HA composite at weeks 4 and 8, red triangle indicating newly formed bone [85], (d2) histological observation of different parts of the implant in the bone environment at 6 months (blue arrows indicate the bones surrounding the implant in the medullary cavity, and white arrows mark the locally corroded site) [86], (d3) histological images showing the maturation of the newly formed bone in Zn-MEM compared to the still unmineralized bone matrix of the Col-MEM group [87]

CHAPTER 2

The material, research methodology and experimental program of the research of this doctoral thesis

2.1 Material and equipment used in the experimental programme

The experimental zinc alloys were developed, cast and prepared for structural investigations in a classical furnace. The mass production of Zn-based alloys is achieved by casting, as this provides easy customization of the alloy composition. Alloy machining by casting involves melting the alloy components, then casting the molten metal into a mold, and finally solidifying. The melting was carried out inside an induction furnace at a temperature generally between 450° and 750 °C depending on the composition of the alloy, The molten metal is cast into a suitable steel or graphite with the desired shape of the ingot for solidification. On the experimental specimens in the tuned state, homogenization heat treatments were performed at 300°C and 400°C, respectively, at each temperature with maintenance of 5 hours and 10 hours. Table 2.1 shows the chemical composition of these experimental alloys.

Table 2.1- Chemical composition of experimental zinc alloys

Alloy	Chemical composition, %Gr.						
	Mg	Fe	S	P	Si	Ni	Zn
Zn	-	-	-	0.019	0.45	0.009	Rest
ZnMg	3.30	-	0.36	0.019	1.06	0.02	rest
ZnMgFe	3.61	1,01	0.3	-	0.72	0.01	rest

2.2 The experimental program carried out within this doctoral thesis

From the experimental specimens developed, specimens were made for the various experiments within the present doctoral thesis. After the structural and mechanical characterization of these specimens, cavitation erosion tests were performed. Biodegradation tests were also carried out from specially cut and specially prepared specimens. In the end, a structural correlation between mechanical behavior and cavitation erosion behavior was achieved, the work ending with original contributions and perspectives for future experimental research . Fig. 2.3 shows the experimental program drawn up in such a way as to lead to the fulfillment of the major objectives initially proposed.

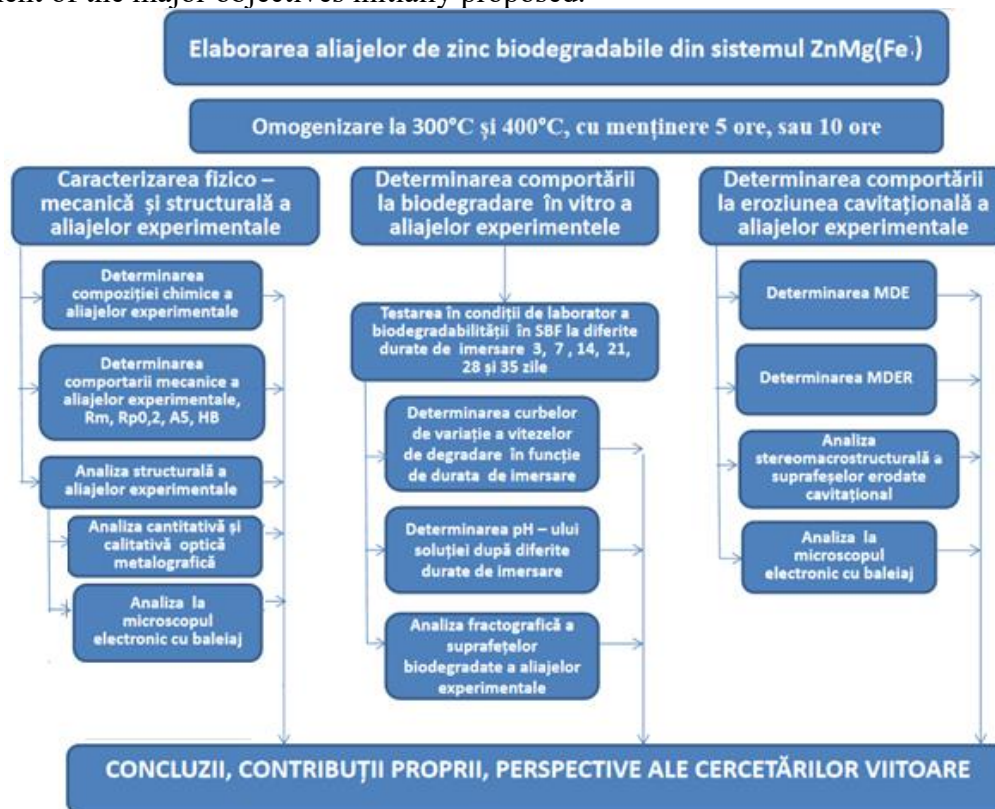


Fig. 2.3- Experimental program of the research within this thesis

CHAPTER 3

PHYSICO-MECHANICAL AND STRUCTURAL CHARACTERIZATION OF EXPERIMENTAL ZINC ALLOYS COMPARED TO PURE ZINC

3.1 Physico-mechanical behavior of zinc alloys in the ZnMg(Fe) system compared to pure zinc

The mechanical behavior of alloys is a particularly important aspect in materials engineering and component design. Thus, in the design and use of alloys, it is important to take into account these mechanical properties to ensure the performance and safety of components made of these materials. This indicates how materials behave under the action of various external forces to which they are subjected. The main relevant mechanical characteristics of metal alloys are:

1. Mechanical strength: This property represents the ability of metals and alloys to oppose external forces that tend to destroy or deform them. These forces can include traction, compression, bending, or twisting. Ductilitatea: Ductilitatea se referă la capacitatea unui material de a se deforma plastic sub acțiunea unei forțe fără a se rupe. Aliajele cu o bună ductilitate pot fi ușor modelate în diverse forme.
2. Toughness measures the ability of a material to absorb energy before it breaks. Tough alloys are important in applications where there is a risk of impact or sudden loading.
3. Fatigue resistance: This refers to the behavior of the material under repeated charging and discharging cycles. Alloys with good fatigue resistance are essential in applications in the aeronautical, automotive and construction industries.
4. Resistance to crack propagation: This property indicates the ability of the material to resist crack growth under the action of stresses. Alloys with good resistance to crack propagation are used in critical components, such as aircraft wings or components of nuclear power plants.

In this chapter, mechanical tests have been carried out in order to mechanically characterize the new experimental alloys, which have different chemical compositions and have been compared with the mechanical characteristics of pure zinc, located in different structural states. The results regarding the mechanical behavior were rendered by presenting both the stress-strain variation curves, as well as by the values of the mechanical characteristics by type of characteristic in the different structural states of the alloys in the form of histograms.

Thus, the stress-strain variation curves of the experimental alloys, as well as those of pure zinc are shown in Fig. 3.1 - Fig. 3.3, and in Table 3.1 are shown the values of the mechanical characteristics resulting from their processing, of zinc and of the experimental zinc alloys.

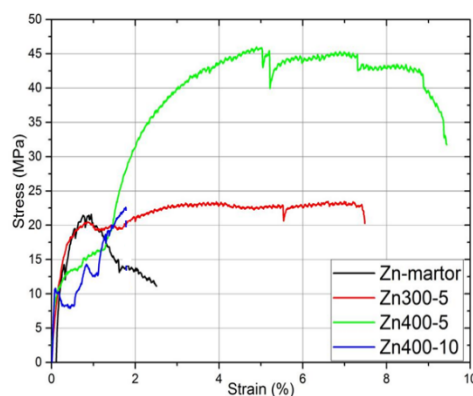


Fig. 3.1-Appearance of the stress-strain tensile curves of pure zinc, in different structural states

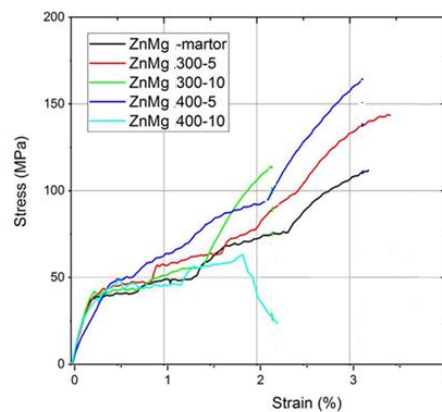


Fig. 3.2-Appearance of the stress-strain tensile curves of ZnMg alloy, in different structural states

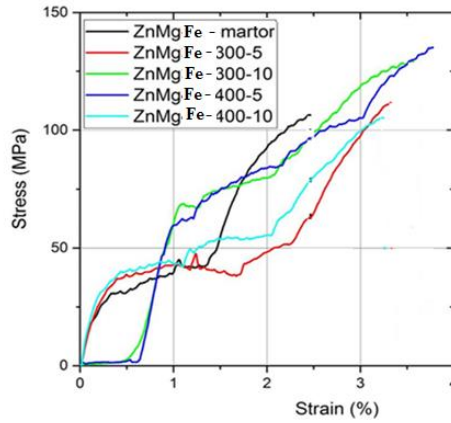


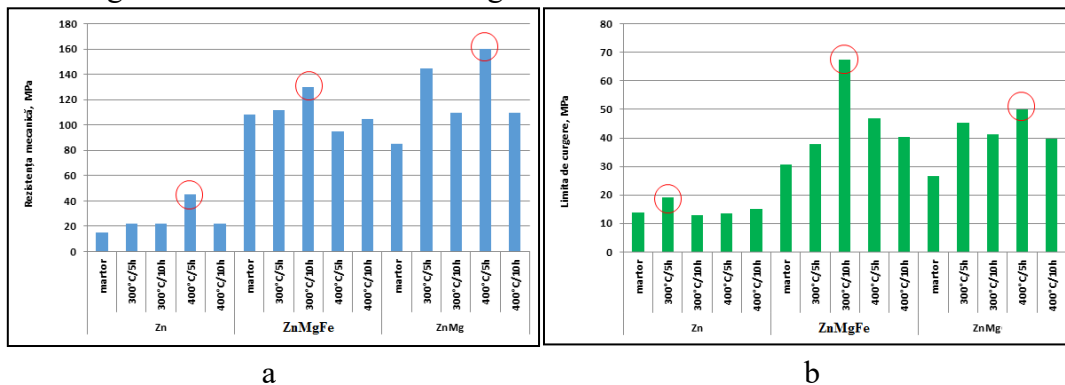
Fig. 3.3-Appearance of the tension-strain tensile curves of ZnMgFe alloy, in different structural states

Table 3.1 - Mechanical characteristics of the zinc alloys investigated in the ZnMg(Fe) system compared to those of pure zinc

Alloy	State	Breaking strength, Rm, (MPa)	Yield Strength, Rp, (MPa)	Elongation at break, A5(%)	Modulus of elasticity, E, (MPa)	Brinell hardness, HB
Zn	pure	15	14	1.8	4.05	22
	300 ^o C/5h	22	19	1.9	9.30	24
	300 ^o C/10h	22	13	2.5	8.30	22
	400 ^o C/5h	45	13.51	2.8	7.26	17
	400 ^o C/10h	22	15.01	1.78	6.50	11
ZnMg	pure	85	26.61	2.66	1.39	48
	300 ^o C/5h	145	45.33	4.23	15.95	76
	300 ^o C/10h	110	41.35	2.16	18.48	57
	400 ^o C/5h	160	50.02	3.14	10.27	62
	400 ^o C/10h	110	39.68	3.22	19.32	68
ZnMgFe	pure	108	30.70	3.69	8.09	74
	300 ^o C/5h	112	37.94	3.32	13.07	75
	300 ^o C/10h	130	67.32	4.13	15.18	32
	400 ^o C/5h	95	46.74	1.92	22.60	76
	400 ^o C/10h	105	40.21	3.25	11.24	77

The comparative analysis on the mechanical behavior of the experimental zinc alloys is presented in the form of histograms in Fig. 3.7

Therefore, it can be concluded that the simple alloy of zinc with magnesium leads to a moderate increase in the values of the mechanical characteristics, while the double alloying of zinc with magnesium and iron leads to a significant increase in the mechanical characteristics



a

b

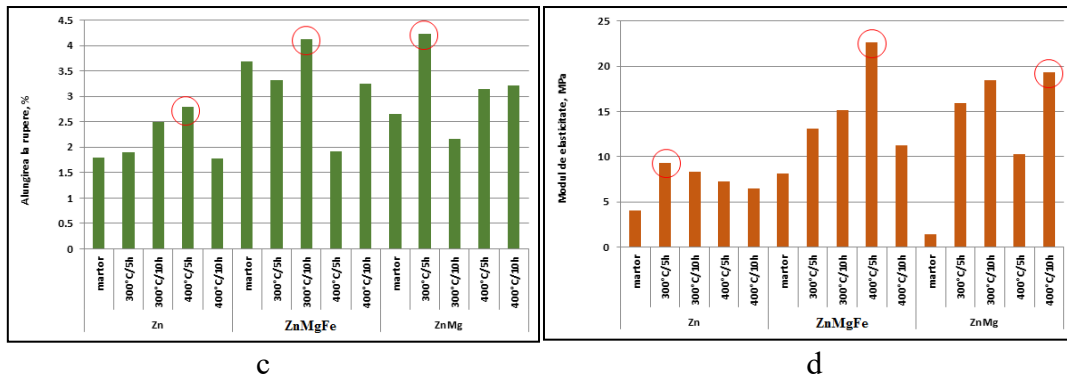


Fig. 3.7- Comparative variation of the mechanical characteristics of the experimental ZnMg(Fe) alloys compared to those of pure zinc: a- mechanical strength, b- yield strength, c- elongation at breakage, d- modulus of elasticity

The macrofractographic analysis of the tensile specimens, performed under the stereomicroscope, both in longitudinal and cross-sectional sections, allowed the evaluation of the fracture surfaces after testing the mechanical characteristics, as well as the critical analysis of the fracture mode of the experimental zinc alloys, compared to pure zinc in different structural states. The stereomicroscope analysis is shown in Fig. 3.8 - Fig. 3.22.

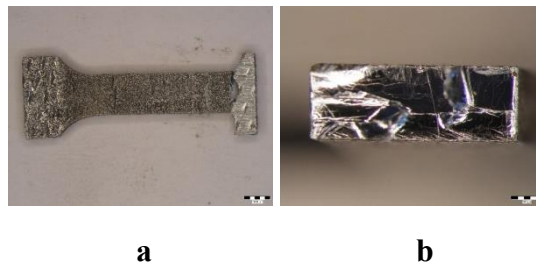


Fig.3.8 - Macroscopic appearance of zinc tensile specimens (control sample): a- longitudinal section, x8; b- cross-section, x40

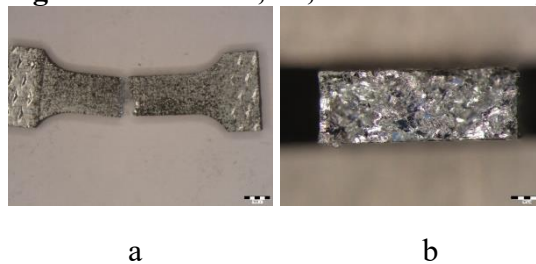


Fig. 3.9-Macroscopic appearance of the Zinc tensile specimens, after annealing at 300°C/5h: a- longitudinal section, x8; b- cross-section, x40

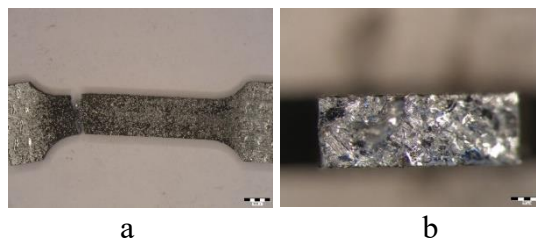


Fig. 3.10-Macroscopic appearance of the Zinc tensile specimens, after annealing at 300°C/10h: a- longitudinal section, x8; b- cross-section, x40

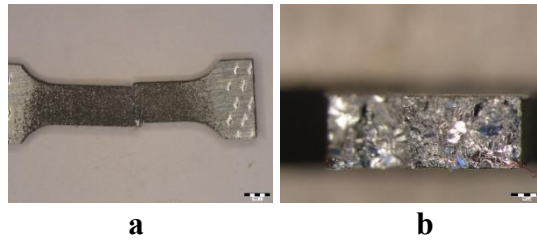


Fig. 3.11-Macroscopic appearance of the Zinc tensile specimens, after annealing at 400°C/ 5h: a- longitudinal section, x8; b- cross-section, x40



Fig. 3.12 - Macroscopic appearance of the zinc tensile specimens, after annealing at 400°C/ 10h: a- longitudinal section, x8; b- cross-section, x40

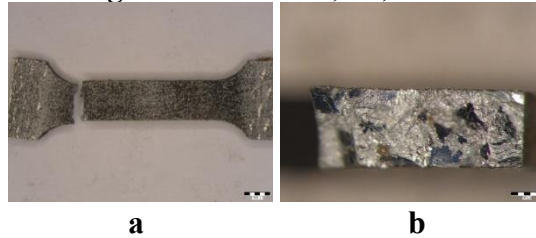


Fig. 3.13-Macroscopic appearance of the ZnMg tensile specimens (control sample):

a- longitudinal section, x8; b- cross-section, x40



Fig. 3.14-Macroscopic appearance of the ZnMg tensile specimens after annealing at 300°C/ 5h: a- longitudinal section, x8; b- cross-section, x40

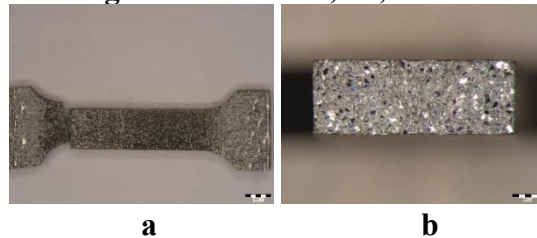


Fig. 3.15-Macroscopic appearance of the ZnMg tensile specimens after annealing at 300°C/ 10h: a- longitudinal section, x8; b- cross-section, x40



Fig. 3.16-Macroscopic appearance of the ZnMg tensile specimens after annealing at 400°C/ 5h: a- longitudinal section, x8; b- cross-section, x40

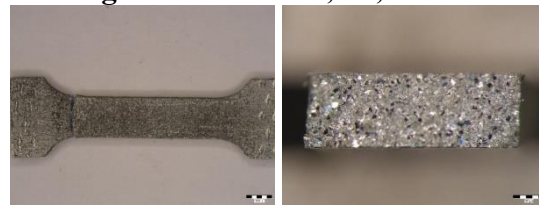


Fig. 3.17-Macroscopic appearance of the ZnMg tensile specimens after annealing at 400°C/ 10h: a- longitudinal section, x8; b- cross-section, x40

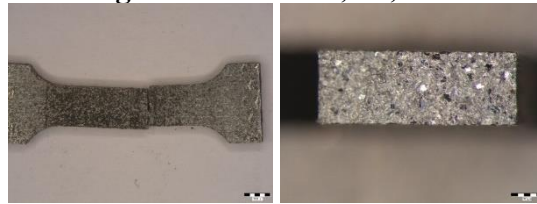


Fig. 3.18-Macroscopic appearance of the ZnMgFe tensile specimens (control sample): a-longitudinal section, x8; b- cross-section, x40

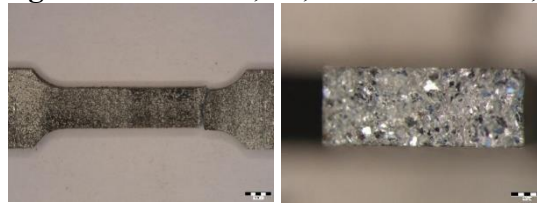


Fig. 3.19-Macroscopic appearance of the ZnMgFe tensile specimens after annealing at 300°C/ 5h: a- longitudinal section, x8; b- cross-section, x40

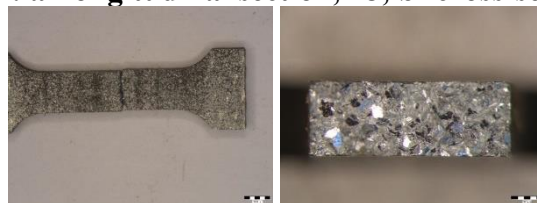


Fig. 3.20-Macroscopic appearance of the ZnMgFe tensile specimens after annealing at 300°C/ 10h: a- longitudinal section, x8; b- cross-section, x40



Fig. 3.21-Macroscopic appearance of the ZnMgFe tensile specimens after annealing at 400°C/ 5h: a- longitudinal section, x8; b- cross-section, x40

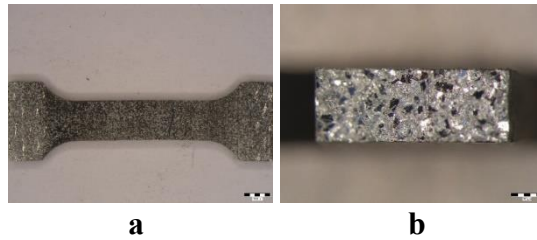


Fig.3.22 - Macroscopic appearance of the ZnMgFe tensile specimens after annealing at 400°C/ 10h: a- longitudinal section, x8; b- cross-section, x40

The structural analysis of the experimental alloys performed under the metallographic light microscope is shown in the figures below:

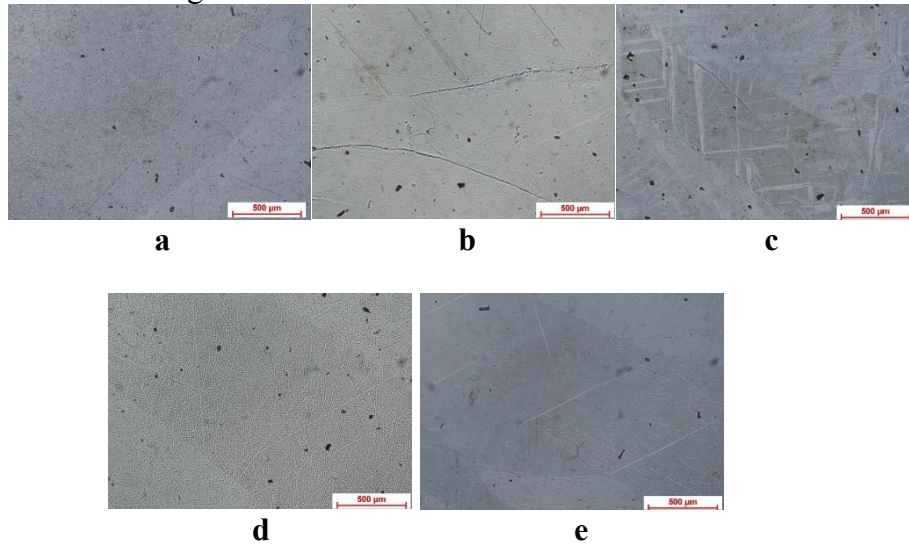


Fig.3.25- Microstructural aspect of Zn: a. control sample; b. after homogenization at 300°C/5h/air; c. after homogenization at 300°C/10h/air; d. after homogenization at 400°C/5h/air; e. after homogenization at 400°C/10h/air

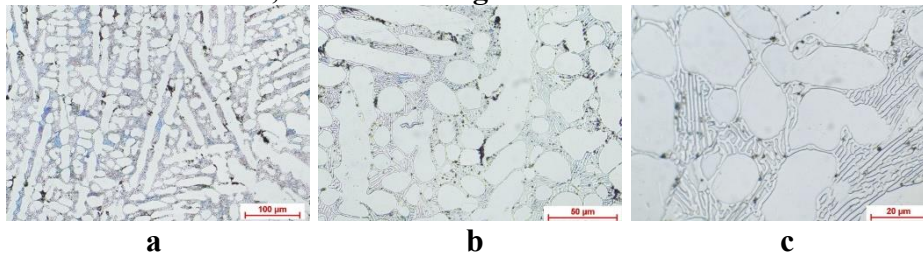


Fig.3.30- Microstructural appearance of the ZnMg alloy, control sample, at different microscope magnification powers

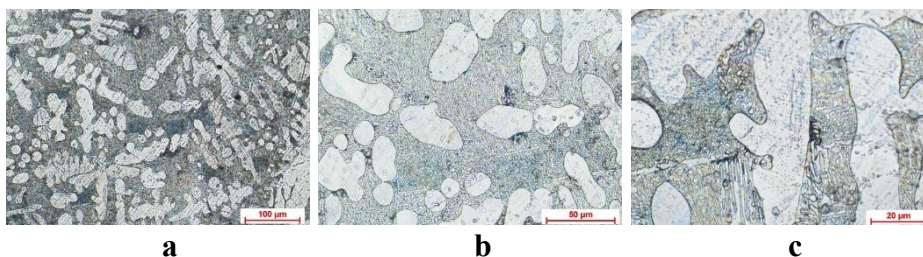


Fig.3.31- Microstructural appearance of the ZnMg alloy, after homogenization at 300°C/5h/air, at different microscope magnification powers

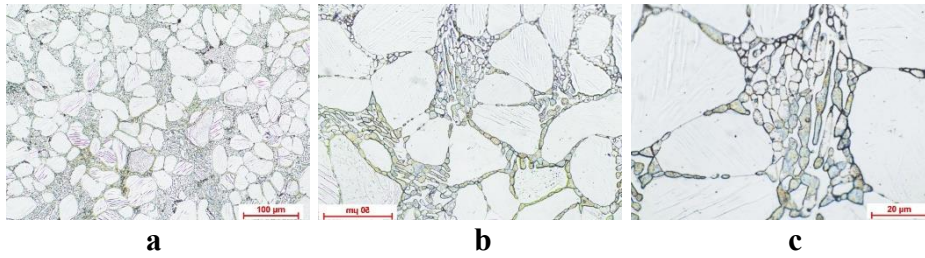


Fig.3.32-Microstructural appearance of the ZnMg alloy, after homogenization at 400°C/10h/air, at different magnification powers of the microscope

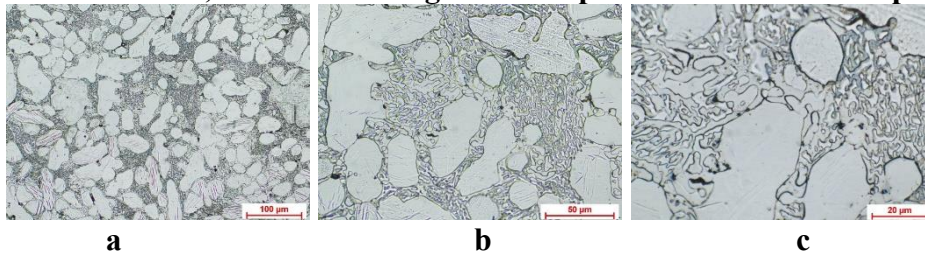


Fig.3.33-Microstructural appearance of the ZnMg alloy, after homogenization at 400°C/5h/air, at different microscope magnification powers

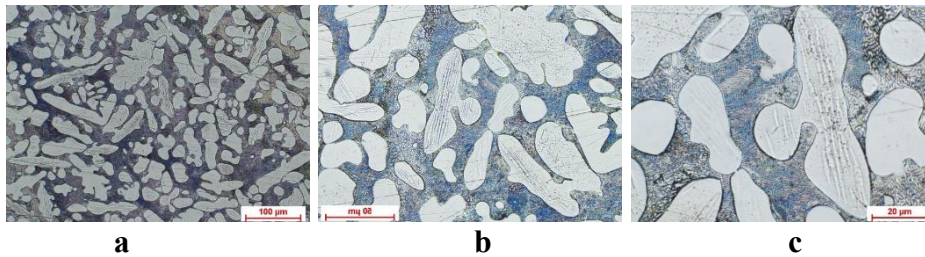


Fig.3.34-Microstructural appearance of the ZnMgFe alloy, control sample, at different magnification powers of the microscope

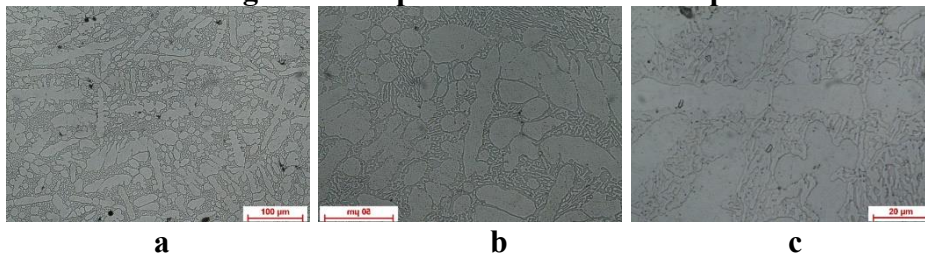


Fig.3.35-Microstructural appearance of the ZnMgFe alloy, after homogenization at 300°C/5h/air, at different microscope magnification powers

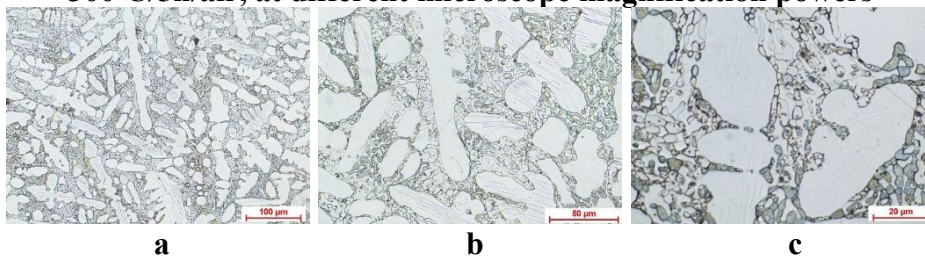


Fig.3.36-Microstructural appearance of the ZnMgFe alloy, after homogenization at 400°C/5h/air, at different magnification powers of the microscope

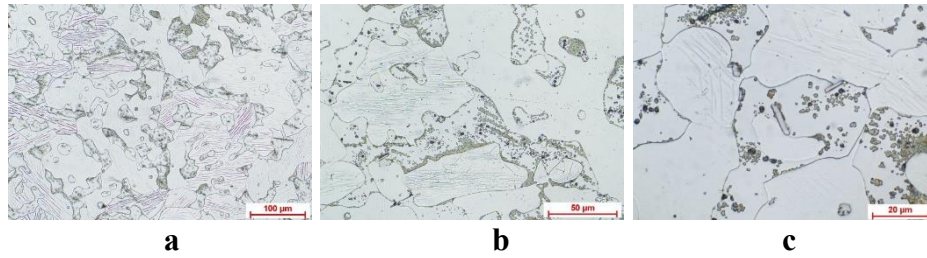


Fig.3.37-Microstructural appearance of the ZnMgFe alloy, after homogenization at 400°C/10h/air, at different microscope magnification powers

3.3 Scanning electron microscope analysis of ZnMg(Fe) alloys.The SEM analysis added information about the nature of shape and the distribution of structural constituents in the biodegradable zinc alloys examined in the paper. The alloying of zinc with essential elements such as magnesium and copper was carried out both to produce alloys with controlled biodegradability and to provide mechanical support for the future biodegradable implant.

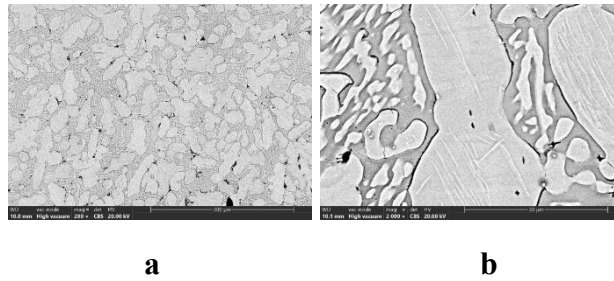
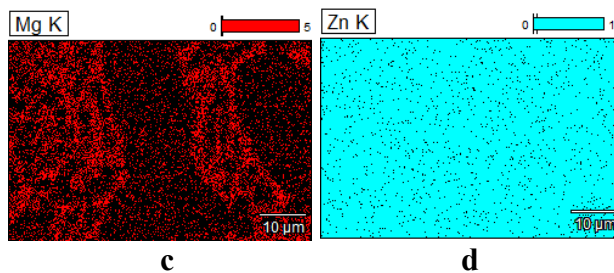
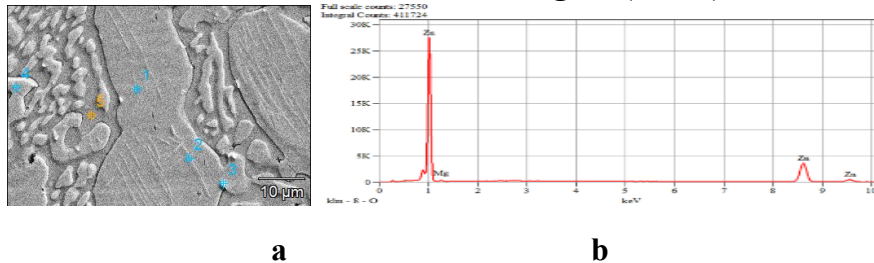


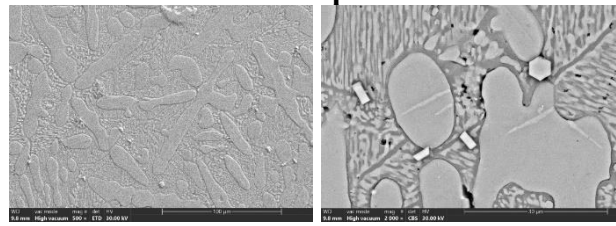
Fig. 3.38- SEM images of the ZnMg alloy, cast state (control sample): A- x1000; b- Detail of image A (x2000)



Zona	Micro-compoziție locală, %gr.	
	Mg	Zn
1	10,2	89,8
2	-	100
3	1,02	98,98
4	4,73	95,27
5	-	100

Fig. 3.39- Analysis of the ZnMg binary alloy under scanning electron microscope:

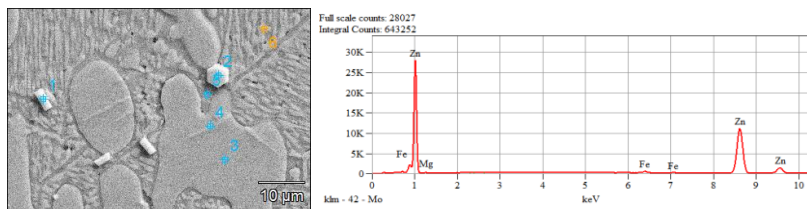
a- SEM image; b- EDAX; c- magnesium distribution; d- zinc distribution; e- Local microcomposition



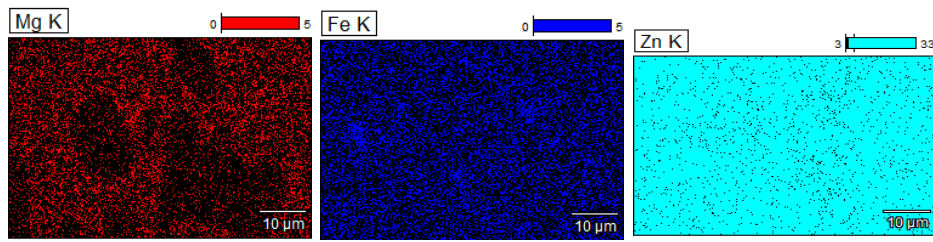
a b

Fig. 3.40- SEM images of the ZnMgFe alloy, cast state (control sample):

a- X1000; b- Detail of image a (x2000)



a b



c d e

Zone	Local micro-composition, %gr.		
	Mg	Fe	Zn
1	1,18	3,43	95,39
2	0,37	1,53	98,1
3	-	-	100
4	-	-	100
5	3,49	-	96,51

f

Fig. 3.41- Analysis of the ZnMgFe binary alloy under scanning electron microscope: a- SEM image; b- EDAX; c- magnesium distribution; d- iron distribution; e- zinc distribution; f- Local microcomposition

CHAPTER 4

Corrosion behavior in human-simulated environments of zinc-based alloys. Corrosion mechanisms and biodegradation behavior

The results regarding the biodegradation behavior of the experimental zinc alloys, compared to pure zinc, in the simulated body fluid, SBF are rendered in the form of graphs regarding the variation of losses in thickness, either intermediate or in absolute value depending on the immersion duration in fig.4.2 and fig.4.3. It can be concluded that the simultaneous alloying of zinc with Mg and Fe determines a better behavior than that of zinc, but inferior to the ZnMg alloy, which has a much more significant degradation.

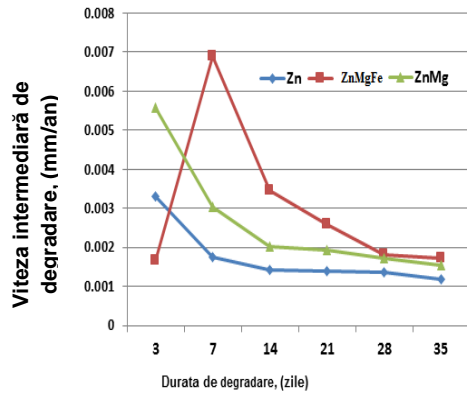


Fig.4.2. - Variation of intermediate degradation rates as a function of degradation duration in SBF of experimental biodegradable zinc alloys in the ZnMg(Fe) system

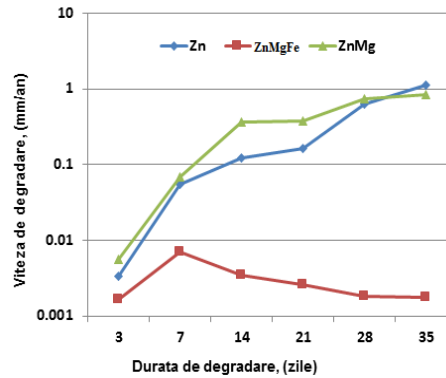


Fig. 4.3. -Variation of absolute degradation rates as a function of degradation time in SBF of experimental biodegradable zinc alloys from the ZnMg(Fe) system

The macrostructural aspects of the degraded surfaces with different immersion durations in SBF, and after the removal of the corrosion products of the alloys are shown in Fig. 4.4 - Fig. 4.6.

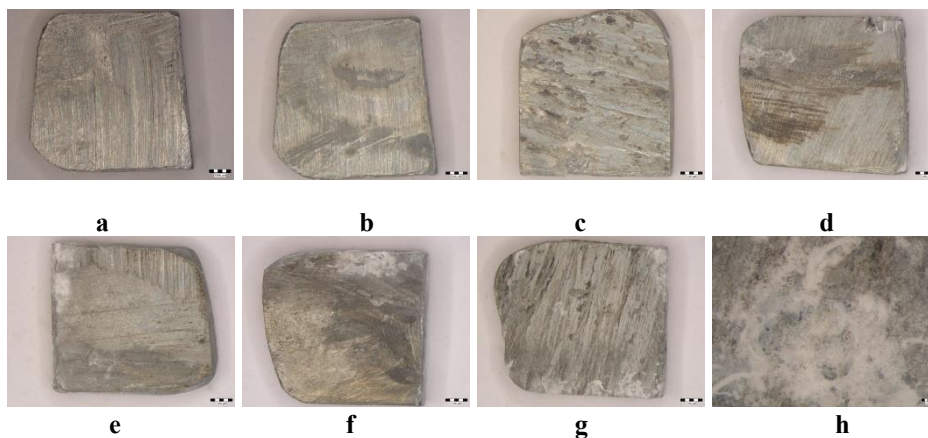


Fig.4.4. - Macrostructural aspects of zinc surfaces degraded in SBF, after different immersion periods, without corrosion products: a- before testing; b- after 3 days; c- after 7 days; d- after 14 days; e- after 21 days; f- after 28 days; g- after 35 days; h- detail of the image g





Fig. 4.5. - Macrostructural aspects of ZnMg alloy surfaces degraded in SBF, after different immersion periods, without corrosion products: a- before testing; b- after 3 days; c- after 7 days; d- after 14 days; e- after 21 days; f- after 28 days; g- after 35 days; h- detail of the image g

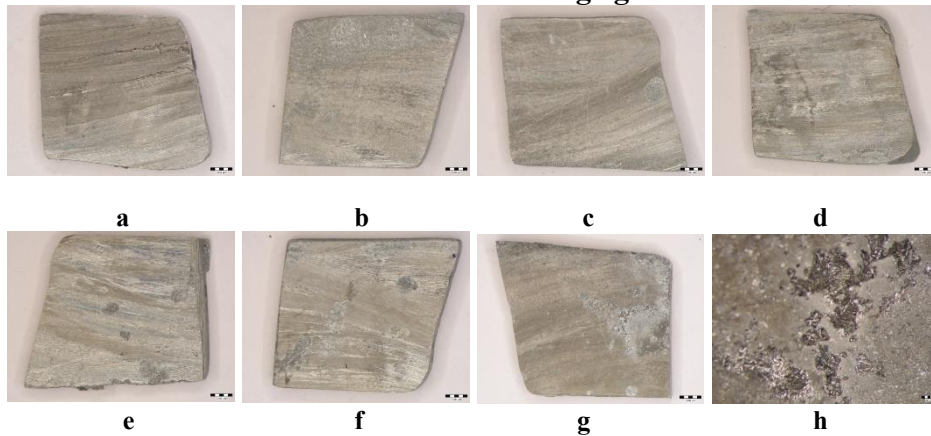


Fig. 4.6.- Macrostructural aspects of ZnMgFe alloy surfaces degraded in SBF, after different immersion periods, without corrosion products: a- before testing; b- after 3 days; c- after 7 days; d- after 14 days; e- after 21 days; f- after 28 days; g- after 35 days; h- detail of the image g

The comparison of the experimental results of the present paper with the data from the literature confirms the fact that the biodegradation behavior of the new zinc-based alloys proposed in this paper is modified by alloying, respectively binary alloys from the ZnMg system and ternary alloys from the ZnMgFe system and, at the same time, the values obtained are comparative and even unexpected for a complex alloy chosen in the paper. Thus: Regardless of the alloying mode, degradation of either zinc or various zinc-based alloys occurs in human-simulated environments [266-280]; The simple alloy of zinc with magnesium causes a significant biodegradation of the alloy from the seventh day of immersion. The appearance of degraded areas after 35 days shows the development of localized degradation areas, with large depths of up to 0.05mm. The absolute degradation rate of the alloy reaches slightly more than 0.002mm/year after 35 days of immersion, [267-282]; The simultaneous alloying of zinc with magnesium and iron causes a behavior similar to that of pure zinc. Biodegradation begins very slowly, from the first removal, 3 days, and continues progressively slowly, until the last 35-day removal. An interconnected network of corrosion points with relatively shallow depths is also noteworthy.

CHAPTER 5



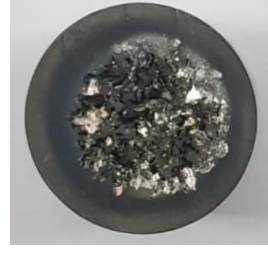

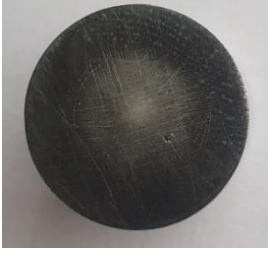


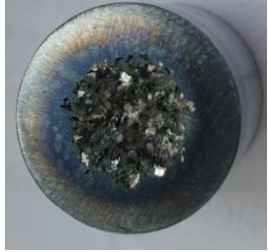
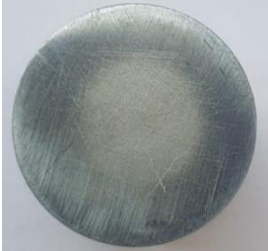

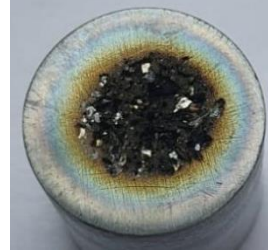



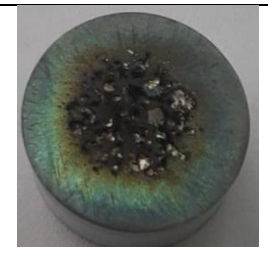

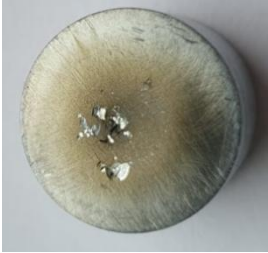
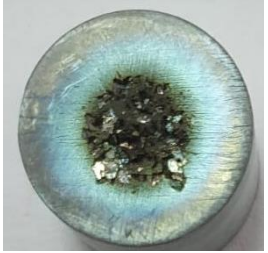


CAVITATIONAL EROSION BEHAVIOR OF EXPERIMENTAL ZINC ALLOYS IN THE ZNMG(Fe) SYSTEM

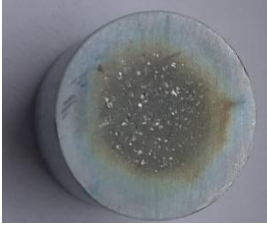
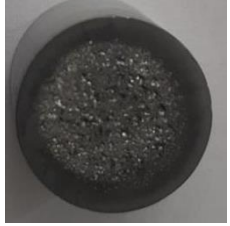






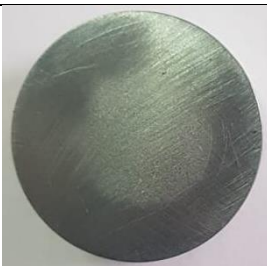
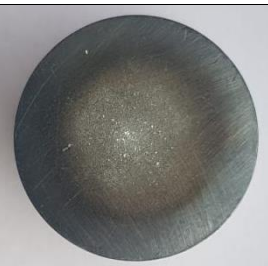














The cavitation erosion behavior of the experimental alloys in the ZnMg(Fe) system was determined by constructing diagrams containing the experimental values of the three samples, tested from each heat treatment state and the specific mediation curves, which give the variation of the average cumulative erosion depth $MDE(t)$ and its velocity $MDER(t)$. They

are the basis for characterizing the behavior and resistance of the surface structure to the erosive stresses of the microjets of vibrating cavitation.

The cavitation attack was followed sequentially at different durations, 15 minutes, 60 minutes, 120 minutes and 165 minutes, respectively, recording the macroscopic aspects in the images shown in Table 5.1.

Table 5.1 - Cavitation attack sequences on cavitated surfaces of specimens in experimental ZnMg(Fe) alloys, in various structural states

Metall/ alloy	state	Duration of cavitation attack, t [min]			
		15	60	120	165
Zn	cast				
	zinc turnat și omogenizat la 300°C/5h				
	zinc turnat și omogenizat la 300°C/10h				
	zinc turnat și omogenizat la 400°C/5h				
	zinc turnat și omogenizat la 400°C/10h				

ZnMg	cast				
	zinc turnat și omogenizat la 300°C/5h				
	zinc turnat și omogenizat la 300°C/10h				
	zinc turnat și omogenizat la 400°C/5h				
	zinc turnat și omogenizat la 400°C/10h				
ZnMgFe	cast				

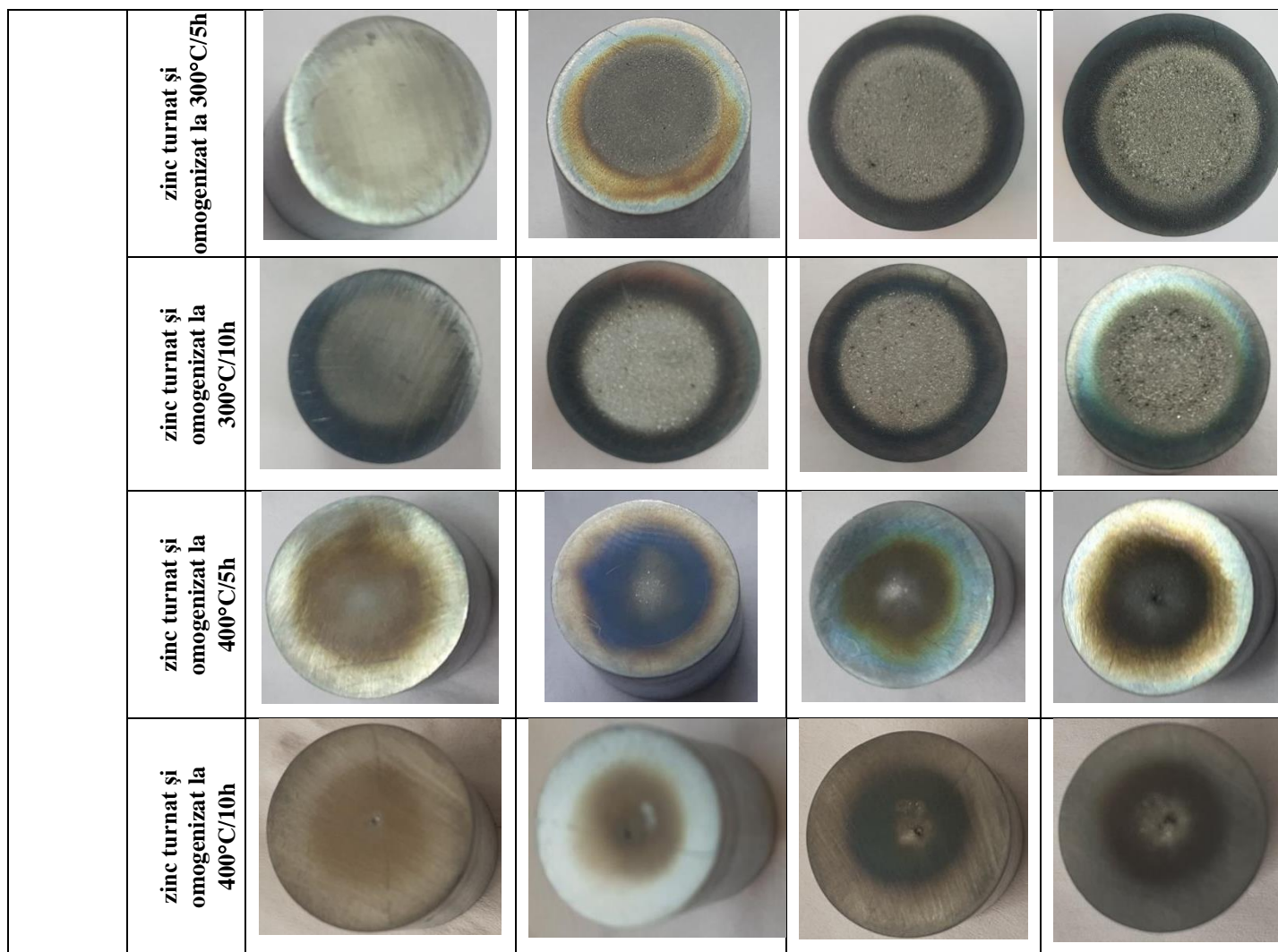


Table 5.2 - Values of statistical parameters recorded during the testing of experimental specimens from experimental alloys of the ZnMg(Fe) system

Alloy	State	Statistical parameters			
		Average erosion penetration depth, MDE _{max} , after 165 minutes of attack [μm]	Maximum value according to the polynomial regression curve [μm]	Minimum value according to the polynomial regression curve [μm]	Standard Estimation Error ()
Zinc	turnat	139,68	120	160	5,451
	zinc turnat și omogenizat la 300°C/5h	38,859	46	29	4,357
	zinc turnat și omogenizat la 300°C/10h	59,746	82	47	7,207
	zinc turnat și omogenizat la 400°C/5h	43,953	49	38	2,86
	zinc turnat și omogenizat la 400°C/10h	39,445	45,5	34	3,064
ZnMg	turnat	30,695	32	28	0.61

	zinc turnat și omogenizat la 300°C/5h	9,441	10	8,8	0.123
	zinc turnat și omogenizat la 300°C/10h	9,922	10,3	9,7	0,294
	zinc turnat și omogenizat la 400°C/5h	13,229	14,2	12	0,921
	zinc turnat și omogenizat la 400°C/10h	15,937	16,3	13,0	1,529
ZnMgFe	turnat	12.651	13.8	12,0	0.272
	zinc turnat și omogenizat la 300°C/5h	9,441	10	8,8	0.123
	zinc turnat și omogenizat la 300°C/10h	7,15	7,8	6,5	0,324
	zinc turnat și omogenizat la 400°C/5h	2,454	2,6	2.3	0,084
	zinc turnat și omogenizat la 400°C/10h	1,25	1,4	1,1	0,042

The comparative analysis of the results regarding the cavitation erosion behavior of the experimental ZnMgFe alloy specimens, in the cast state and various homogenization treatments at 300°C or 400°C, with maintenance durations of 5 hours, 10 hours, allowed the synthesis of the results in the histogram in fig. 5.18.

Table 5.3 Quantitative analysis of surfaces subjected to cavitation attack of experimental test specimens made of ZnMg(Fe) alloys in different structural states

Alloy	Cast Status	Diameters			Proportions	
		Exterior, μm	Intermediar, μm	Interior, μm	Total area affected by cavitation attack, %	Surface most affected by cavitation attack, %
Zn	turnat	15928	44872	11039	75	69
	zinc turnat și omogenizat la 300°C/5h	16115,7	11783,3	9214,3	73	57
	zinc turnat și omogenizat la 300°C/10h	15981,3	11066,3	9467,0	69	59
	zinc turnat și omogenizat la 400°C/5h	15904	10419	9059	66	57
	zinc turnat și omogenizat la 400°C/10h	15998	9897	9170	61	57
ZnMg	turnat	15876	14916	12174	94	77
	zinc turnat și omogenizat la 300°C/5h	15835	11859	10721	75	68

	zinc turnat și omogenizat la 300°C/10h	15842	12773	11219	81	71
	zinc turnat și omogenizat la 400°C/5h	15873	10629	9453	67	60
	zinc turnat și omogenizat la 400°C/10h	15820	10705	9416	68	60
ZnMgFe	turnat	15925	15192	12834	95	81
	zinc turnat și omogenizat la 300°C/5h	16024	12091	10141	75	63
	zinc turnat și omogenizat la 300°C/10h	15952	12695	9658	78	61
	zinc turnat și omogenizat la 400°C/5h	15866	12358	10704	78	67
	zinc turnat și omogenizat la 400°C/10h	15910	9334	4194	59	26

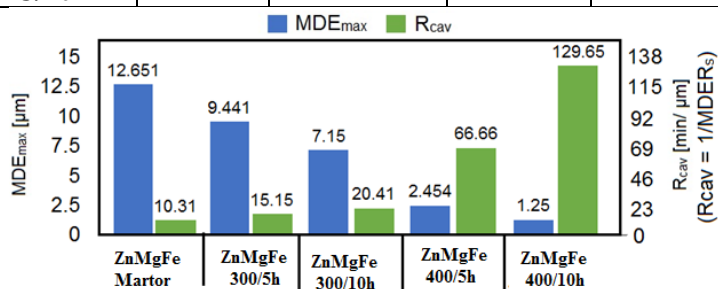


Fig. 5.18 Histogram of the comparison of the results regarding the cavitation erosion behavior of experimental specimens made of ternary ZnMgFe alloys, casting and various homogenization heat treatments

So, it can be concluded: alloying with magnesium leads to an increase of up to 7 times in the cavitation resistance of zinc; Simultaneous alloying with magnesium and iron increases the cavitation resistance of zinc by more than 100 times

CHAPTER 6

FRACTOGRAPHIC ANALYSIS OF CAVITATIONALLY ERODED SURFACES OF EXPERIMENTAL SPECIMENS MADE OF BIODEGRADABLE ALLOYS FROM THE ZnMg(Fe) system

In the present paper it was intended to perform a detailed fractographic analysis under the scanning electron microscope, on the one hand to identify the characteristics of the fracture propagation mode caused by cavitation attack, in general, on biodegradable zinc alloy surfaces, in particular, and, on the other hand, to distinguish between the different fracture

modes, correlated with the structural condition of the metallic material. It can also be highlighted that a fractographic analysis of biodegradable zinc alloy surfaces subjected to attack by cavitation erosion is an innovative objective of this scientific research paper. The fractographic analysis under the scanning electron microscope of the experimental specimens of the experimental biodegradable zinc alloys, in different structural states required at cavitation after 165 hours of immersion, highlighted the erosion of the surfaces and is shown in fig. 6.1 ÷ fig. 6.6, allowing the formulation of the following aspects.

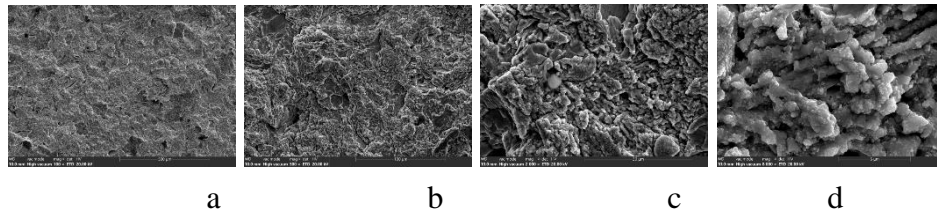


Fig.6.1- SEM images of cavitationally eroded zinc specimens, after 165h, at different magnification powers: a- x100; b- x500; c- x2000; d- 8000x

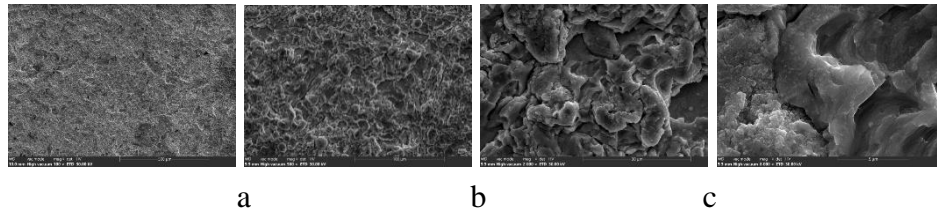


Fig.6.2- SEM images of cavitationally eroded zinc specimens, after aging at 400°/10/air, after 165h, at different magnification powers: a- x100; b- x500; c- x2000; d- 8000x

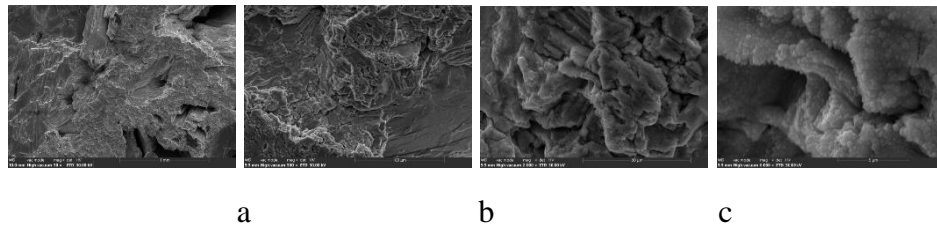


Fig.6.3- SEM images of cavitationally eroded ZnMg alloy specimens, after 165h, at different magnification powers: a- x50; b- x500; c- x2000; d- 8000x

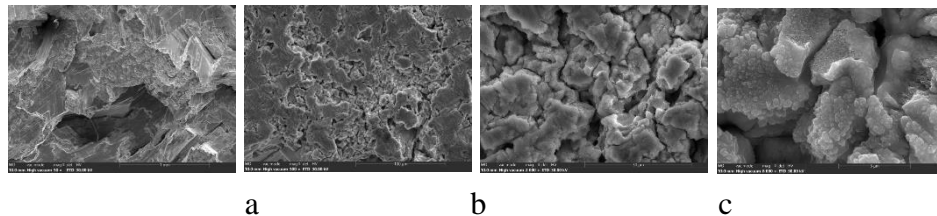


Fig. 6.4- SEM images of cavitationally eroded specimens made of ZnMgFe alloy, after 165h, and aging at 400°C/10h/air, at different magnification powers: a- x50; b- x500; c- x2000; d- 8000x

CHAPTER 7 - CONCLUSIONS. ORIGINAL CONTRIBUTIONS. PROSPECTS FOR FUTURE RESEARCH

ORIGINAL CONTRIBUTIONS

- Creation of new zinc alloys with superior biodegradation properties from ZnMg binary systems and ZnMgFe ternary systems, which differ from those investigated so far in the literature and have well-defined chemical compositions;
- Detailed examination of the physico-mechanical and structural characteristics of the new biodegradable zinc alloys, respectively from the binary system ZnMg and the ternary system ZnMgFe, as well as the realization of a structural correlation of the way in which the different alloying elements, respectively magnesium and iron, influence their mechanical behavior.
- Determination of the cavitation erosion behavior of the new biodegradable zinc alloys, respectively from the ZnMg binary system and the ZnMgFe ternary system, a behavior not yet studied in the literature. Also, through the study carried out on specimens in different structural states, casting and casting and homogenization at 300°C and 400°C with maintenance at 5 hours or 10 hours, it was possible to achieve a correlation between the structural characteristics of the investigated alloys in the binary system ZnMg and the ternary system ZnMgFe and the behavior to cavitation erosion;
- Laboratory testing of new zinc alloys for biodegradation behavior, respectively alloys from the binary system ZnMg and the ternary system ZnMgFe, in human simulant liquid (SBF) at different immersion durations, respectively 3, 7, 14, 21, 28 and 35 days, behavior not yet studied in the literature. Variation curves were also made to compare the results by degradation rate and pH as a function of immersion duration. The experimental results of this work, compared with the data from the literature, allow to highlight the influence of the alloying elements, respectively magnesium and cumulative iron, on the biodegradation behavior of zinc-based alloys;
- Fractographic analysis of cavitationaly eroded surfaces from the newly proposed experimental alloys, respectively alloys from the ZnMg binary system and from the ZnMgFe ternary system, an analysis not performed so far in the literature. Through the study carried out, it was possible to highlight the mechanism of the erosion phenomenon at cavitation corrosion, under the conditions of compositional changes by alloying these alloys;
- Initial examination of cavitationaly eroded surfaces using quantitative stereomacrostructural analyses on the proposed new compositions, respectively alloys from the ZnMg binary system and the ZnMgFe ternary system, an examination not yet performed in the literature. The extension of both the total cavitationaly attacked surface and the most cavitationaly attacked surface is noteworthy. Consequently, the total areas affected by cavitation erosion in newly proposed alloys in the cast state are approximately 60%, while in alloys that have been homogenized they are up to 70%.
- Cast alloys also have the surfaces most affected by cavitation attack lower, at about 55 to 50%, while homogenized alloys have up to 60%. By performing these analyses, it is possible to enrich the database, both in the field of stereomacrostructural analysis and in the field of biodegradable zinc alloys in ZnMg(Fe) systems.

BIBLIOGRAPHY

- Antoniac, I.; Miculescu, M.; Mănescu, V.; Stere, A.; Quan, P.H.; Păltânea, G.; Robu, A.; Earar, K. Magnesium-Based Alloys Used in Orthopedic Surgery. *Materials* **2022**, *15*, 1148.
- Antoniac, I.V.; Filipescu, M.; Barbaro, K.; Bonciu, A.; Birjega, R.; Cotrut, C.M.; Galvano, E.; Fosca, M.; Fadeeva, I.V.; Vadalà, G.; et al. Iron Ion-Doped Tricalcium Phosphate Coatings Improve the Properties of Biodegradable Magnesium Alloys for Biomedical Implant Application. *Adv. Mater. Interfaces* **2020**, *7*, 2000531
- I Antoniac, V Manescu, A Antoniac, G Paltanea, Magnesium-based alloys with adapted interfaces for bone implants and tissue engineering, *Regenerative Biomaterials* *10*, rbad095
- I Antoniac, V Manescu, G Paltanea, A Antoniac, IV Nemoianu, MI Petrescu, Additive manufactured magnesium-based scaffolds for tissue engineering, *Materials* *15* (23), 8693
- B Yuan, H Chen, R Zhao, X Deng, G Chen, X Yang, Z Xiao, A Aurora, Construction of a magnesium hydroxide/graphene oxide/hydroxyapatite composite coating on Mg–Ca–Zn–Ag alloy to inhibit bacterial infection and promote bone regeneration, *Bioactive materials* *18*, 354–367, 62, 2022
- H Chen, B Yuan, R Zhao, X Yang, Z Xiao, A Aurora, BA Iulia, X Zhu, Evaluation on the corrosion resistance, antibacterial property and osteogenic activity of biodegradable Mg-Ca and Mg-Ca-Zn-Ag alloys, *Journal of Magnesium and Alloys* *10* (12), 3380–3396
- Rau, J.V.; Antoniac, I.; Filipescu, M.; Cotrut, C.; Fosca, M.; Nistor, L.C.; Birjega, R.; Dinescu, M. Hydroxyapatite Coatings on Mg-Ca Alloy Prepared by Pulsed Laser Deposition: Properties and Corrosion Resistance in Simulated Body Fluid. *Ceram. Int.* **2018**, *44*, 16678–16687.
- Antoniac, I.; Miculescu, F.; Cotrut, C.; Ficai, A.; Rau, J.V.; Grosu, E.; Antoniac, A.; Tecu, C.; Cristescu, I. Controlling the Degradation Rate of Biodegradable Mg–Zn–Mn Alloys for Orthopedic Applications by Electrophoretic Deposition of Hydroxyapatite Coating. *Materials* **2020**, *13*, 263.
- R Adam, I Antoniac, S Negoită, C Moldovan, E Rusu, C Orban, In Vivo Study of Local and Systemic Responses to Clinical Use of Mg–1Ca Bioresorbable Orthopedic Implants, *Diagnostics* *12* (8), 1966
- Quan, P.H.; Antoniac, I.; Miculescu, F.; Antoniac, A.; Manescu, V.; Robu, A.; Bița, A.I.; Miculescu, M.; Saceleanu, A.; Bodog, A.D.; et al. Fluoride Treatment and In Vitro Corrosion Behavior of Mg–Nd–Y–Zn–Zr Alloys Type. *Materials* **2022**, *15*, 566.
- Streza, A.; Antoniac, A.; Manescu, V.; Paltanea, G.; Robu, A.; Dura, H.; Verestiuc, L.; Stanica, E.; Voicu, S.I.; Antoniac, I.; et al. Effect of Filler Types on Cellulose-Acetate-Based Composite Used as Coatings for Biodegradable Magnesium Implants for Trauma. *Materials* **2023**, *16*, 554.
- Bița, A.-I.; Antoniac, I.; Miculescu, M.; Stan, G.E.; Leonat, L.; Antoniac, A.; Constantin, B.; Fornă, N. Electrochemical and In Vitro Biological Evaluation of Bio-Active Coatings Deposited by Magnetron Sputtering onto Biocompatible Mg–0.8Ca Alloy. *Materials* **2022**, *15*, 3100.
- V Manescu, I Antoniac, A Antoniac, D Laptoiu, G Paltanea, R Ciocoiu, Bone Regeneration Induced by Patient-Adapted Mg Alloy-Based Scaffolds for Bone Defects: Present and Future Perspectives, *Biomimetics* *8* (8), 618
- A Streza, A Antoniac, R Ciocoiu, CM Cotrut, M Miculescu, F Miculescu, In Vitro Studies Regarding the Effect of Cellulose Acetate-Based Composite Coatings on the Functional Properties of the Biodegradable Mg3Nd Alloys, *Biomimetics* *8* (7), 526
- L Dragomir, A Antoniac, V Manescu, A Robu, M Dinu, I Pana, CM Cotrut, Preparation and characterization of hydroxyapatite coating by magnetron sputtering on Mg–Zn–Ag alloys for orthopaedic trauma implants, *Ceramics International* *49* (16), 26274–26288
- L Dragomir, I Antoniac, V Manescu, A Antoniac, M Miculescu, O Trante, Microstructure and corrosion behaviour of Mg-Ca and Mg-Zn-Ag alloys for biodegradable hard tissue implants, *Crystals* *13* (8), 1213
- T Bită, A Antoniac, I Ciuca, M Miculescu, CM Cotrut, G Paltanea, H Dura, Effect of fluoride coatings on the corrosion behavior of Mg–Zn–Ca–Mn alloys for medical application, *Materials* *16* (13), 4508

• LIST OF PUBLISHED WORKS

Articole ISI web of knowledge

1. **Gheorghe Cristina Maria**, Petre Gabriela; Trante, Octavian; Milea Claudia Georgiana; Ghiban, Brandusa -CORROSION BEHAVIOUR OF ZAMAK COMPONENTS IN A HEARING AID, UNIVERSITY POLITEHNICA OF BUCHAREST SCIENTIFIC BULLETIN SERIES B-CHEMISTRY AND MATERIALS SCIENCE, Volume 83, Issue 4, Page, 251-262
2. GABRIELA CIUNGU, LAVINIA MADALINA MICU, ILARE BORDEASU, CRISTINA MARIA IORDACHE, BRANDUSA GHIBAN, CRISTIAN GHERA- RESEARCH OF THE CAVITATION RESISTANCE OF A BIODEGRADABLE ALLOY Zn-Cu, U.P.B. Sci. Bull., Series ..., Vol. ..., Iss. ..., 201 ISSN 1223-7027 (in curs de publicare)

BDI Listed Items

3. **Iordache (Gheorghe) Cristina Maria**, Nicolae Alexandru Luca, Bordeasu Ilare, Ciungu Gabriela, Ghiban Brandusa - Cavitation Erosion Behavior of a Biodegradable Alloy from the Zn-Mg System for Biomedical Applications, *Tribology in Industry*, DOI: 10.24874/ti.1548.09.23.11, 2024, 46(2), pp. 315–323,
4. Luca Nicolae Alexandru, Bordeasu Iordache, **Iordache (Gheorghe) Cristina Maria**, Miculescu Marian, Madalina Micu- Heat Treatment Influence on the Cavitation Erosion Zn-Mg Behavior Used for Biomedical Applications, *Tribology in Industry*, DOI: 10.24874/ti.1604.11.23.01, 2024, 46(2), pp. 270–282

Papers presented at national conferences/ international participation

1. Brândușa Ghiban, Iulian Vasile Antoniac, Cristina Maria Iordache, Gabriela Petre, Aurora Antoniac New biodegradable zinc alloys for biomedical applications , BIOMAH 2024 (Roma)
2. Iordache (Gheorghe) Cristina Maria, Nicolae Alexandru Luca, Bordeasu Ilare, Ciungu(Petre) Gabriela, Ghiban Brandusa - Cavitation Erosion Behavior of a Biodegradable Alloy from the Zn-Mg System for Biomedical Applications- on-line presentation, SERBIATRIB'23, 18th International Conference on Tribology
3. Luca Nicolae Alexandru, Bordeasu Iordache, Iordache (Gheorghe) Cristina Maria, Miculescu Marian, Madalina Micu- Heat Treatment Influence on the Cavitation Erosion Zn-Mg Behavior Used for Biomedical Applications, on-line presentation SERBIATRIB'23, 18th International Conference on Tribology
4. C.M. Iordache (Gheorghe), G.Cingiu(Petre), B.Ghiban- Structural modifications in ZnMg(Ca) alloys for orthopedic applications , ROMAT 2022
5. G. Ciungu (Petre), C.M. Iordache (Gheorghe), B. Ghiban - Structural modifications in ZnCu(Mg) alloys for cardiovascular applications, ROMAT 2022
6. Gabriela Ciungu, Cristina Maria Iordache, Robert Ciocoiu, Brandusa Ghiban- Structural characterization of a new ZnCu(Mg) biodegradable alloy, BioReMed 2023
7. Cristina Maria Iordache, Gabriela Ciungu, Marian Miculescu, Robert Ciocoiu, Brandusa Ghiban-Heat Treatment Influence on The Mechanical and Structure properties of a new ZnMg(Ca) biodegradable alloy, BioReMed 2023